J. Hydrol. Hydromech., 68, 2020, 1, 60–69
DOI: 10.2478/johh-2019-0027
ISSN 1338-4333

sciendo Journal of Hydrology and Hydromechanics

Collisional transport model for intense bed load

Václav Matoušek*, Štěpán Zrostlík

Czech Technical University in Prague, Department of Civil Engineering, Thákurova 7, 166 29 Prague 6, Czech Republic.
* Corresponding author. E-mail: v.matousek@fsv.cvut.cz

Abstract: In an open channel with a mobile bed, intense transport of bed load is associated with high-concentrated sediment-laden flow over a plane surface of the eroded bed due to high bed shear. Typically, the flow exhibits a layered internal structure in which virtually all sediment grains are transported through a collisional layer above the bed. Our investigation focuses on steady uniform turbulent open-channel flow with a developed collisional transport layer and combines modelling and experiment to relate integral quantities, as the discharge of solids, discharge of mixture, and flow depth with the longitudinal slope of the bed and the internal structure of the flow above the bed.

A transport model is presented which considers flow with the internal structure described by linear vertical distributions of granular velocity and concentration across the collisional layer. The model employs constitutive relations based on the classical kinetic theory of granular flows selected by our previous experimental testing as appropriate for the flow and transport conditions under consideration. For given slope and depth of the flow, the model predicts the total discharge and the discharge of sediment. The model also predicts the layered structure of the flow, giving the thickness of the dense layer, collisional layer, and water layer. Model predictions are compared with results of intense bed-load experiment carried out for lightweight sediment in our laboratory tilting flume.

Keywords: Granular flow; Sheet flow; Sediment transport; Grain collision; Tilting flume experiment; Kinetic theory.

INTRODUCTION

For intense bed load transport in an open channel with a mobile bed, collisional interactions of transported sediment grains are typical and they significantly affect behavior of flow carrying the sediment above a plane mobile bed at high bed shear (the upper-stage bed regime). The flow exhibits a layered structure in which virtually all grains are transported through a collisional transport layer. If the total bed shear stress exerted by the flow is high, a sliding dense layer develops between the collisional layer and the bed. In the dense layer, grains remain in virtually permanent contact and slide over each other rather than collide with each other. Typically, the collisional layer dominates the internal structure of the flow. Appropriate modelling of friction and transport in the layered structure of the flow is crucial for prediction ability of a bed-load transport model. So far, collisional mechanisms are poorly understood and hence modelling approaches are seldom sufficiently accurate.

Most widely used transport formulae are simple and semi-empirical by nature (e.g., Cheng, 2002; Meyer-Peter and Müller, 1948; Rickenmann, 1991; Smart, 1984; Wilson, 1966; Wong and Parker, 2006). They employ only integral quantities of the flow and do not take the internal structure of the flow into account.

One of the appropriate theory-based approaches to modelling of flows dominated by granular collisions seems to be the kinetic theory of granular flows. It offers constitutive relations for local shear-induced collision-based granular quantities – normal stress, shear stress and fluctuation energy - and relate them with distribution of local grain concentration and velocity across the flow depth. Kinetic-theory based models enable a prediction of relevant flow quantities in the layered pattern of the flow. Model predictions include integral flow quantities (discharges of solids and mixture, flow depth) and simplified distributions of solids concentration and velocity.

Typically, a kinetic-theory based model assumes certain conditions at interfaces of the layered flow and quantifies the interfacial stresses, concentration, and velocity. Additional equations (momentum balances) are employed to use the interfacial values of the granular quantities for the prediction of thicknesses of the relevant layers. The discharges of solids and mixture are obtained through integration of the velocities and concentrations over the flow depth. The existing models differ mainly in assumptions taken for the layered flow and in forms of the constitutive relations selected for the models (e.g., Berzi, 2011; Berzi and Fraccarollo, 2013; Capart and Fraccarollo, 2011; Spinewine and Capart, 2013).

In our previous work (Matoušek and Zrostlík, 2018a), results from a tilting-flume facility including measured velocity distribution and deduced concentration distribution (approximated as linear profiles) were used to calculate distributions of the collision-based quantities by the constitutive relations and hence to test the ability of the selected kinetic-theory constitutive relations to predict conditions observed in these collision-dominated flows.

In this paper, we aim on formulating a simple kinetic-theory-based model using the constitutive relations previously tested for flow conditions observed in our intense-bed-load experiment in a laboratory tilting flume.

TRANSPORT MODEL FOR COLLISIONAL BED LOAD IN OPEN-CHANNEL FLOW OF LAYERED STRUCTURE

A modelling approach is discussed which enables to predict characteristics of steady uniform turbulent open-channel flow carrying a large amount of colliding sediment (intense bed-load). The approach is based on the classical kinetic theory, considers a layered structure of the sediment-laden flow and employs conditions at layer interfaces to evaluate mutual relations among the flow slope, depth, the thickness of the layers and flow rates of both the sediment and sediment-water mixture. In the discussed model, the dense limit condition consider-

ing the local volumetric concentration $c \rightarrow 1$ (see a discussion on this condition in Matoušek and Zrostlík (2018a)) is not assumed at the bottom of the collisional transport layer because our experiments indicate that for the studied flow conditions the local concentration at the bottom of the collisional layer is too low to satisfy the dense limit condition (Matoušek et al., 2016).

Modelled conditions for open-channel flow and sediment transport

- Gravity-driven open-channel flow, steady-state uniform turbulent flow.
- Broad range of bed slopes, flows depths, sediment flow rates, and total flow rates.
- Flow over mobile bed at upper-stage plane bed regime (high bed shear).
- Transported sediment grains supported by mutual contacts, negligible turbulent support.
- Strongly non-uniform distribution of sediment across the flow depth.
- Stratified flow as the result of the sediment distribution.

It is typical of flows with intense bed load transport that local concentrations and velocities of grains span a broad range of values over the thickness of the collisional layer. As mentioned previously, it is also typical that the collisional layer dominates the layered structure of the flow and occupies a considerable part of the flow depth. Figure 1 shows the layered character of flow with intense bed-load identified for flow of mixture of water and lightweight sediment in a laboratory flume (plastic cylinder-shaped grains of the characteristic size of 5.41 mm and the density of 1307 kg/m^3). It recognizes the following distinct layers: the bed (stationary deposit with the surface expressed as the 0-boundary in Figure 1), the dense sliding layer (DL, with the top d-boundary), the collisional layer (CL, with the upper c-boundary), and the water layer (WL, with water surface at the top of the plot in Figure 1). Visual observations of the flow and measurements of local velocities u at different vertical positions y above the bed allowed the layer boundaries to be identified. The CL (the layer of colliding grains) exhibits the velocity distribution which can be approximated by a line reaching virtually zero velocity at the bottom of CL and this identifies the position of the d-boundary. Hence, the velocity of grains in the DL (the dense layer of grains slowly sliding over each other and being in permanent contact with each other) is negligible compared to velocities in the CL. Above the top of the CL no grains occur, which identifies the c-boundary.

Two plots of Figure 1 are for two flows of different values of the bed Shields parameter θ_0, which is the dimensionless total shear stress at the surface of the bed (i.e., at the 0-boundary), $\theta_0 = \dfrac{\tau_{e,0}}{\left(\rho_s - \rho_f\right) \cdot g \cdot d}$ ($\tau_{e,0}$ = the total shear stress at the surface of the bed, ρ_s = density of grains, ρ_f = density of liquid, g = gravitational acceleration, and d = grain size). The plots show that the thickness of individual layers varies with θ_0. At low values of θ_0, the thickness of the dense layer is negligible but can reach a thickness of the multiple of the grain size d at very high θ_0. Furthermore, an analysis of measured discharges suggested that the local volumetric concentration at the bottom of collisional layer, c_d, was smaller than the bed volumetric concentration, c_0, and varied with θ_0 until a certain maximum value typical for bed was reached (Matoušek et al., 2016).

The existence of the individual layers, the variation of their thickness and of the conditions at the boundaries must be taken into account in the transport model.

Model principles

The conditions subject to modelling require that the model is based on principles describing the collisional character of sediment transport. Different forms of constitutive relations are available in the literature. As tested in a laboratory (Matoušek and Zrostlík, 2018a), the constitutive relations of the classical kinetic theory (CKT) below are appropriate for our modelled conditions. The testing revealed that for the conditions given by our experiments, the constitutive relations worked well if the local volumetric concentration of sediment did not exceed approximately 0.47. Furthermore, the experimental results showed that the local concentration at the bottom of the collisional transport layer varied with the bed shear stress and reached values smaller than 0.47 in most of flow conditions observed. Therefore, the use of the constitutive relations at this boundary is appropriate, at least in the range of bed shear stresses for which the modelled flow conditions and model assumptions are satisfied. Also, the testing of the constitutive relations showed that the application of the dense limit condition is not appropriate due to these relatively low values of the local concentration even though it meant that more complex forms of the relations have had to be solved at the bottom of the collisional layer.

CKT considers sheared granular bodies, in which grains are supported exclusively by mutual binary collisions. The constitutive relations are formulated for local grain stresses (normal and shear) and for a balance of grain fluctuation energy in the collisional regime.

The local shear-induced granular normal stress, σ_s, is related to the local volumetric concentration of grains, c, the local granular temperature, T (which expresses a measure of local grain velocity fluctuations due to intergranular collisions), and after the theory by Garzo and Dufty (1999) as in Berzi (2011),

$$\sigma_s = 4 \cdot \rho_s \cdot f_\sigma \cdot c \cdot G \cdot T \tag{1}$$

where G, f_σ = concentration-related functions defined as

$$G = c \cdot \frac{2 - c}{2 \cdot \left(1 - c\right)^3} \tag{2}$$

$$f_\sigma = \frac{1 + e}{2} + \frac{1}{4 \cdot G} \tag{3}$$

where e = the coefficient of wet restitution (local values of e may vary with position above bed).

The local shear-induced granular shear stress, τ_s, is also related to c and T at any vertical position y above the bed. Moreover, τ_s is related to the local strain rate γ_s, i.e. the distribution of longitudinal velocity of grains u_s ($\gamma_s = \mathrm{d}u_s/\mathrm{d}y$), (Berzi, 2011),

$$\tau_s = \rho_s \cdot f_\tau \cdot c \cdot G \cdot \sqrt{T} \cdot \gamma_s \cdot d \tag{4}$$

with concentration-related function

$$f_\tau = \frac{8}{5 \cdot \sqrt{\pi}} \cdot \left(\frac{1 + e}{2} + \frac{\pi}{32} \cdot \frac{\left[5 + 2 \cdot (1 + e) \cdot (3 \cdot e - 1) \cdot G\right] \cdot \left[5 + 4 \cdot (1 + e) \cdot G\right]}{\left[24 - 6 \cdot (1 - e)^2 - 5 \cdot \left(1 - e^2\right)\right] \cdot G^2} \right) \tag{5}$$

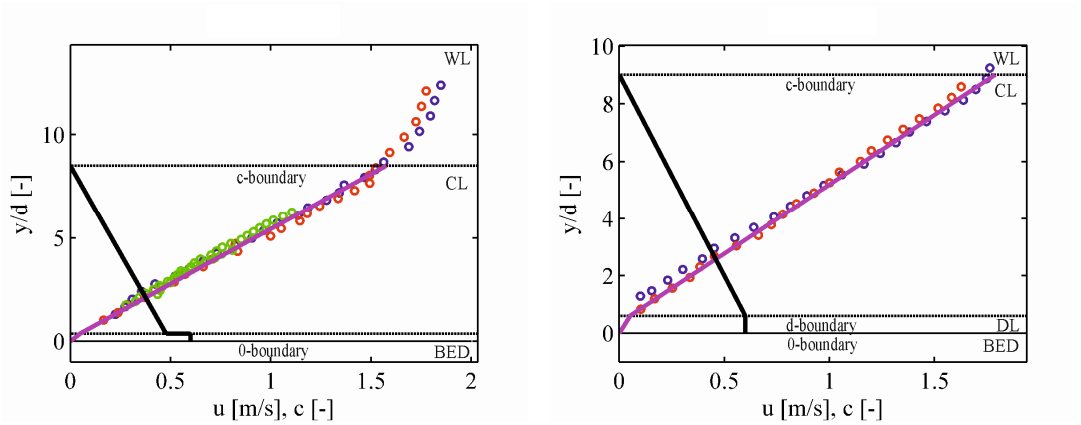

Fig. 1. Positions of boundaries, velocity and concentration profiles in layered-structure flow carrying plastic (TLT50) grains. Legend: circle – measurement of local velocity by different measuring techniques (blue – Pitot tube, red – Ultrasonic Velocity Profiler, green – Acoustic Doppler Velocitometer); horizontal lines – boundaries between layers (bed, DL = dense layer, CL = collisional layer, WL – water layer); thick lines – velocity profile by local velocity approximation and concentration profile deduced from measurement (Matoušek and Zrostlík, 2018b).

Another constitutive relation expresses the balance of the particle collisional fluctuation energy. It requires that the gradient of the vertical component of the flux of particle fluctuation energy balances the net rate of production of fluctuation energy per unit volume of the mixture (Jenkins and Hanes, 1998). The relation is composed of three terms. The first term represents the diffusion of fluctuation energy, the second term the production of energy due to shearing, and the third term represents the rate of collisional dissipation, i.e. the fluctuation energy dissipated by interparticle collisions (Armanini et al., 2005). For our conditions, the diffusion term can be neglected in the lower part of the collisional layer (Matoušek and Zrostlík, 2018a) and the kinetic-energy relation becomes an additional equation relating the granular shear stress with the granular temperature and the strain rate,

$$\tau_s = \frac{24}{\sqrt{\pi}} \cdot \rho_s \cdot c \cdot G \cdot (1-e) \cdot \frac{\sqrt{T^3}}{\gamma_s \cdot d} \tag{6}$$

Alternative equations relating the distribution of the local concentration with the distributions of the granular stresses are based on the principle of momentum balance. In gravity-driven solid-liquid flow with a free surface, the force balance between the driving force and the resisting force assumes that the total shear stress, τ_e (composed of the granular component, τ_s, and the liquid component, τ_f) at each vertical position y balances the longitudinal component of the weight of overlaying burden of liquid and solids,

$$\tau_e = g \cdot \sin\omega \cdot \int_y^H \left[\rho_s \cdot c + \rho_f \cdot (1-c)\right] \cdot dy \tag{7}$$

in which ω = angle of longitudinal slope of bed, and H = total flow depth.

The granular normal stress balances the normal component of the submerged weight of grains above y,

$$\sigma_s = (\rho_s - \rho_f) \cdot g \cdot \cos\omega \cdot \int_y^H c \cdot dy \tag{8}$$

It follows from re-arrangements of Eqs. (7) and (8) that

$$\tau_e = \sigma_s \cdot \tan\omega + \rho_f \cdot g \cdot \sin\omega \cdot (H - y) \tag{9}$$

where the first term on the right-hand side of Eq. (9) is the granular component, τ_s, of the total shear stress and the second term is the liquid component, τ_f.

Model features

Semi-empirical transport formulae for bed load relate the solids discharge with the shear stress at the top of the mobile bed. A kinetic-theory based model can serve the same purpose by relating the granular shear stress at the bottom of the collisional layer with relevant flow quantities responsible for the solids discharge. Furthermore, an incorporation of the momentum balance equations allows to capture the layered structure of the flow and to identify positions of the layer boundaries. For chosen (e.g. experimentally determined) input quantities, the model does not require the classical law of the wall to relate the total discharge with the flow depth.

In the presented model, the constitutive relations of the classical kinetic theory are employed to describe granular flow conditions at the bottom of the CL, where the local concentration is supposed to vary with the boundary shear stress. The constitutive relations also predict the slope of the linear profile of solids velocity in the CL and hence they determine the local velocity u_c at the top of the CL. The momentum balances are combined with the shear-to-normal stress ratios at the relevant boundaries to determine positions of the boundaries in the layered flow structure. The discharges of solids and mixture are obtained through integration of the velocities and concentrations over the flow depth.

Model assumptions

- Distribution of velocity and concentration linear in the CL, concentration distribution uniform and solids velocity negligible in the DL. Local concentration zero at the top of CL (c-boundary). These assumptions are in an agreement with conditions observed in Figure 1.
- Negligible fluid stress at the d-boundary and at the 0-boundary.
- No side-wall effect.
- No local slip between grain and liquid in the CL and DL.
- The diffusive term of the energy-balance relation is negligible at the d-boundary (and 0-boundary).

Set of model governing equations

The model is composed of the following set of equations (constitutive relations, momentum balances, and closures). The situation at the bottom of the collisional layer (the d-boundary) is central to the modelling procedure. The constitutive relations for stresses at this boundary are formulated as follows. The shear induced normal granular stress (based on Eq. (1) with G- and f_σ-functions by Eqs. (2) and (3), respectively) is

$$\sigma_{s,d} = 4 \cdot \rho_s \cdot f_{\sigma,d} \cdot c_d \cdot G_d \cdot T_d \tag{10}$$

the corresponding granular shear stress (based on Eq. (4) with the f_τ-function by Eq. (5)) is

$$\tau_{s,d} = \rho_s \cdot f_{\tau,d} \cdot c_d \cdot G_d \cdot \sqrt{T_d} \cdot \gamma_{s,d} \cdot d \tag{11}$$

and the same shear stress expressed from the energy balance with negligible diffusion term as in Eq. (6) is

$$\tau_{s,d} = \frac{24}{\sqrt{\pi}} \cdot \rho_s \cdot c_d \cdot G_d \cdot (1 - e_d) \cdot \frac{\sqrt{T_d^3}}{\gamma_{s,d} \cdot d} \tag{12}$$

The local coefficient of restitution at the bottom of the CL, e_d, equals (e.g., Berzi and Fraccarollo, 2013)

$$e_d = \varepsilon - 62.1 \cdot \frac{\mu_f \cdot (1 + \varepsilon)}{\rho_s \cdot \sqrt{T_d} \cdot d} \tag{13}$$

in which ε = effective coefficient of dry collisional restitution (a material constant, which is a model input parameter), μ_f = dynamic viscosity of fluid.

At the d-boundary, the granular stresses are mutually related through the friction coefficient

$$\beta_d = \frac{\tau_{s,d}}{\sigma_{s,d}} \tag{14}$$

and its value is determined by Eq. (14) from the obtained values of both stresses in the model.

The momentum balance equations based on Eqs. (8) and (9) relate the local stresses at the d-boundary with the and local concentration c_d, and the positions the d-boundary, y_d, and c-boundary, y_c,

$$\sigma_{s,\mathrm{d}} = (\rho_s - \rho_f) \cdot c_d \cdot g \cdot \cos\omega \cdot (y_c - y_d) / 2 \tag{15}$$

$$\tau_{e,d} = \tau_{e,c} + \sigma_{s,d} \cdot \tan\omega + \rho_f \cdot g \cdot \sin\omega \cdot (y_c - y_d) \tag{16}$$

Similarly, Eqs. (8) and (9) applied to the 0-boundary (the top of the bed, $y_0 = 0$) produce

$$\sigma_{s,0} = \sigma_{s,d} + (\rho_s - \rho_f) \cdot c_0 \cdot g \cdot \cos\omega \cdot y_d \tag{17}$$

$$\tau_{e,0} = \tau_{e,d} + (\sigma_{s,0} - \sigma_{s,d}) \cdot \tan\omega + \rho_f \cdot g \cdot \sin\omega \cdot y_d \tag{18}$$

where the local concentration at the 0-boundary, c_0, is one of the input constants of the model.

At the bottom of the flow (the 0-boundary), the Coulomb yield criterion requires

$$\beta_0 = \frac{\tau_{s,0}}{\sigma_{s,0}} \tag{19}$$

and its value is another input constant of the model.

At the top of the collisional layer (the c-boundary), the total shear stress is entirely due to fluid shearing (the local solids stress is zero) and hence following Eq. (9),

$$\tau_{e,c} = \rho_f \cdot g \cdot \sin\omega \cdot (H - y_c) \tag{20}$$

The linear distribution across the CL leads to

$$u_{s,c} = u_{s,d} + \gamma_{s,d} \cdot (y_c - y_d) \tag{21}$$

Linear distributions of u_s and c across the CL (with assumed $c_c = 0$, $u_{s,d} = 0$) are combined with the earlier determined positions of the boundaries to give the sediment discharge (Matoušek et al. 2016),

$$q_s = \frac{c_d \cdot u_{s,c} \cdot (y_c - y_d)}{6} \tag{22}$$

If the assumptions of no slip in the CL and of the uniform velocity distribution in the WL are taken, then the total discharge (mixture of sediment and liquid) is

$$q_m = \frac{u_{s,c} \cdot (y_c - y_d)}{2} + u_{s,c} \cdot (H - y_c) \tag{23}$$

The average spatial volumetric concentration of sediment in the flow cross section is

$$C_{vi} = \frac{c_0 \cdot y_d + c_d / 2 \cdot (y_c - y_d)}{H} \tag{24}$$

Summary of model constants, input and output variables

In general, there are 4 mutually related major quantities characterizing the sediment-laden flow: the longitudinal slope of bed, ω, the flow depth, H, the sediment discharge, q_s, and the mixture discharge, q_m. To be able to compare model predictions with experimental results of flume tests (as the test results in Figure 1), we use the measured bed slope and the measured thickness of CL, y_c-y_d, as inputs and predict the flow depth and the two discharges. Alternatively, the model can consider the flow depth as an input and to predict the thickness of the CL. Additional model outputs are the position of the top of the DL, y_d, the velocity at the top of the CL, $u_{s,c}$, and the granular-stress ratio at the bottom of the CL, β_d. Additional model inputs are the concentrations c_d, and c_0, the properties of solids (ρ_s, d) and fluid (ρ_f, μ_f), the coefficient of internal friction at the top of bed, β_0, and the dry restitution coefficient, ε.

DISCUSSION OF TRANSPORT MODEL AND COMPARISON OF MODEL PREDICTIONS WITH EXPERIMENTAL RESULTS

For a comparison of model predictions with experimental data, the model version was used with the thickness of the CL as an input to the model and the flow depth as one of the model outputs. The experimental values of (y_c–y_d) and c_d were used as inputs to initialize model calculations. The model flow chart in Figure 2 visualizes the model calculation procedure further described in the paragraph below.

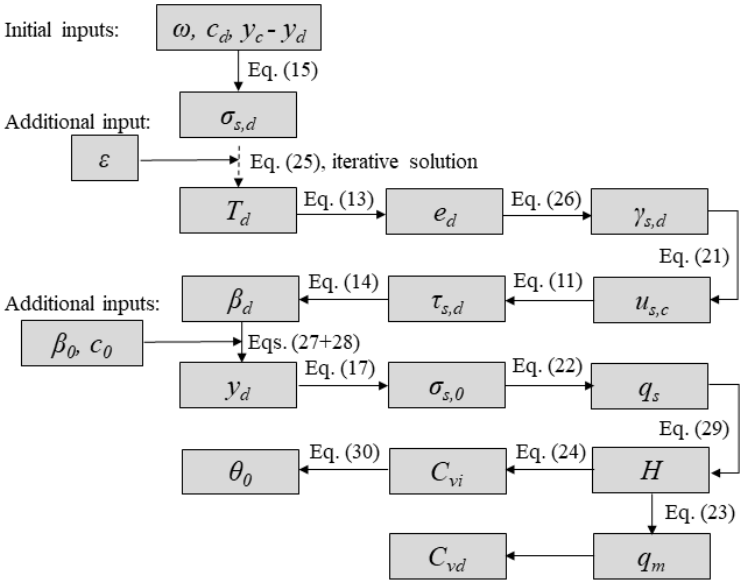

Fig. 2. Model flow chart.

Model calculation for CL-thickness as input and flow depth as output

Eq. (15) calculates the solids normal stress at the d-boundary, $\sigma_{s,d}$. The CKT-based relations (Eqs. (10) and (13)) combined produce an iterative solution for the granular temperature at the d-boundary,

$$T_d = \frac{\sigma_{s,d}}{4 \cdot \rho_s \cdot f_{\sigma,d}(T_d) \cdot c_d \cdot G_d} \tag{25}$$

For the obtained T_d, the two shear-stress constitutive relations (Eqs. (11) and (12)) combined give the velocity gradient at the d-boundary,

$$\gamma_{s,d} = \sqrt{\frac{24 \cdot (1-e_d) \cdot T_d}{\sqrt{\pi} \cdot f_{\tau,d} \cdot d^2}} \tag{26}$$

The linear distribution of velocity is assumed in the CL above the d-boundary and thus the gradient remains constant across the entire CL. The momentum balance equations for the 0-boundary (Eqs. (17) and (18)) together with the equations for the friction coefficients at the 0-boundary and d-boundary (Eqs. (14) and (19)) and the assumption of zero fluid shear stresses at the two boundaries leads to the relation for the thickness of the dense layer,

$$y_d = \frac{(\beta_0 - \beta_d) \cdot \sigma_{s,d}}{\rho_0 \cdot g \cdot \sin\omega - \beta_0 \cdot (\rho_0 - \rho_f) \cdot g \cdot \cos\omega} \tag{27}$$

in which the local density of mixture at the 0-boundary,

$$\rho_0 = \rho_f + (\rho_s - \rho_f) \cdot c_0 \tag{28}$$

A combination of shear-stress balances at the d-boundary and c-boundary (Eqs. (16) and (20) together with Eq. (14)) leads to the determination of the total flow depth,

$$H = y_d + \frac{\sigma_{s,d} \cdot (\beta_d - \tan\omega)}{\rho_f \cdot g \cdot \sin\omega} \tag{29}$$

Then Eq. (24) calculates C_{vi} using H and both quantities can be further employed to express the bed Shields parameter, i.e. the dimensionless total shear stress at the 0-boundary, as

$$\theta_0 = \left(C_{vi} + \frac{\rho_f}{\rho_s - \rho_f} \right) \cdot \frac{H}{d} \cdot \tan\omega \tag{30}.$$

Comparison of model predictions with experimental results

Experimental results for 4 fractions of plastic grains of different sizes and shapes (Table 1) are compared with predictions of the model. The experimental results were collected in our tilting flume and the data, the procedure of their collection and processing and the experimental set-up itself are described elsewhere (e.g., Matoušek at al., 2016).

The properties the sediment fractions produce values of the particle Reynolds number ($\mathrm{Re}_p = \mathrm{v_t d / v_f}$) $\mathrm{Re}_p = \rho_f \cdot v_t \cdot d_{eq} / \mu_f$ in the range from 416 to 1149 and the flow conditions correspond with values of the bed Shields parameter from 0.3 to 1.6. The absence of local turbulent support of grains in the collisional layer is checked by determining a distribution of the velocity ratio u_f^*/v_t (u_f^* is the fluid shear velocity, $u_f^* = \sqrt{\tau_f / \rho_f}$) across the CL for each test run (examples are shown in Matoušek and Zrostlík (2019)). Local values were always below unity and typically smaller than 0.8, indicating that the turbulent support can be neglected. This argument is supported by regime maps (Fig. 7 in Berzi and Fraccarollo (2013) and Fig. 6 in Berzi and Fraccarollo (2016)) in which our flows collapsed in the collisional regime. The experimental conditions were similar to those used previously by other authors for testing their bed-load transport models (Armanini et al., 2005; Berzi and Fraccarollo, 2013; Capart and Fraccarollo, 2011).

For all sediment fractions, the model predictions are obtained with the same values of the model constants ($\beta_0 = 0.55$, $c_0 = 0.55$), in an exception of values of the restitution coefficient ε. The ε values are summarized in Table 1 and the table indicates that the required different values are associated with the different shapes of grains of the different fractions. The better agreement is reached between the predictions and the experimental results if cylindrical grains, i.e. the grains of the height comparable with the diameter of the cylinder (TLT50 and FA60) are given a lower value of ε than the lens-shaped grains for which the height is approximately one half of the lens diameter (TLT25 and FA30).

From the total collected dataset, only those experimental data were selected which corresponded with the model assumption that the local concentration at the top of the collisional layer is zero ($c_c = 0$). Some of the flume experiments were carried out for saturated flows in which sediment particles occupied the entire flow depth. Hence, the water layer was nonexistent and the local concentration of particles was considerable even at positions just below the water surface. This was the case for flows of the highest values of the Shields parameter θ_0, and such flows were excluded from the comparison with model predictions.

The velocity and concentration distributions of the experimental test runs were processed using the procedure described in Matoušek et al. (2016) and the positions of the boundaries and local concentrations at the boundaries were produced. Figures 3 and 4 show the experimentally determined values of the concentration c_d (Figure 3) and of the relative thickness of the collisional layer $(y_c - y_d)/d$ (Figure 4). As discussed previously, values of these two parameters are among the model inputs, although the thickness of the CL can be replaced by the flow depth H as a model input. Note, that the experimentally determined values of c_d and y_d are both quite sensitive to θ_0, as Figures 3 and 4 demonstrate.

The thickness of the dense layer (represented by y_d) is predicted by the model using Eq. (27). Although the dense layer tends to be very thin (typically up to 2 or 3 layers of grains at very high θ_0) and unimportant from the point of view of sediment transport (usually the transport through the layer is negligible), apparently the variation in its thickness indicates the variation in c_d and this variation is important for the overall transport (see e.g., Matoušek and Zrostlík, 2018b).

The parity plots of Figure 5 indicate how successful is the model in a prediction of the local velocity at the top of the collisional layer. The model captures the velocity $u_{s,c}$ (obtained from Eq. (21)) reasonably well over the entire range of the observed flow conditions.

Values of the predicted flow depth H (calculated by Eq. (29)) prove the model's ability to successfully transform the prediction of the internal structure of the flow into the prediction of integral quantities of the mixture flow and sediment transport as is the depth H in Figure 6 and other important integral quantities shown in Figures 7 and 8. For the predicted depth H, the agreement is again reasonable although less strong than is the agreement with the experiments for the predicted discharge of sediment q_s shown in Figure 7.

The ratio of two flow-depth averaged concentrations is evaluated in Figure 8. The delivered concentration of sediment is defined and determined as $C_{vd} = q_s/q_m$ (using results from Eqs. (22) and (23)). Its value must be smaller than the corresponding value of the spatial volumetric concentration C_{vi} (Eq. (24)) and it is indeed the case for all results in Figure 8. Furthermore, a predicted value of the concentration ratio C_{vd}/C_{vi} is sensitive to predicted values of all other integral quantities (q_s, q_m, H) and to predicted values of the local quantities (velocities and concentrations at all boundaries). Hence, it is an interesting parameter for an overall evaluation of the model performance. The degree of the agreement is very similar for this ratio as for the quantities presented in the previous figures.

In overall, the results of model predictions are satisfactory, although a bigger body of experimental results is required to make the validation more general, particularly including results for natural solids like sand and gravel. Moreover, additional work is required to further sophisticate the model, e.g., by finding out whether the observed variation of c_d with the transport conditions could be captured by the model instead of taking it as model input information.

To finalize, the proposed way of modelling of the steady-state uniform open-channel sediment-laden (bed-load) flow is compared with the traditional way. It considers only integral parameters and requires two equations to predict 2 of the 4 mutually related major quantities (ω, H, q_s, q_m). Those equations are the momentum equation for mixture flow and the transport formula for the sediment transport. The momentum equation (typically Chezy equation) includes a solution for the boundary friction (the law-of-the-wall formula for bed friction coefficient). The Meyer-Peter and Müller transport formula is often used for bed load transport. Usually, the slope ω and the flow depth H are the inputs and the sediment discharge q_s is obtained from the transport formula and the mixture discharge q_m from the momentum equation. In principle, the here proposed model serves the same purpose (predicts 2 major quantities using the other 2 as inputs) and besides the properties of solids and liquid requires just a few additional constants (ε, β_0, c_0). There is one another input parameter, c_d, which cannot be considered constant and its value must be estimated or obtained by experiment.

Table 1. Properties of model sediment fractions of lightweight (PVC plastic) grains.

Experimentally determined values	TLT50	TLT25	FA60	FA30
Density ρ_s (kg/m^3)	1307	1381	1411	1368
Shape of grains	cylinder	thick lens	cylinder	thick lens
Height of cylinder or lens (mm)	5.0	2.2	5.0	2.2
Diameter of cylinder or lens (mm)	4.8	4.8	6.1	4.0
Equivalent mass-median diameter d_{eq} (mm)	5.41	4.23	6.42	3.65
Terminal settling velocity of grain v_t (m/s)	0.149	0.106	0.179	0.114
Estimated values of model constant	TLT50	TLT25	FA60	FA30
Restitution coefficient ε (–)	0.70	0.85	0.60	0.85

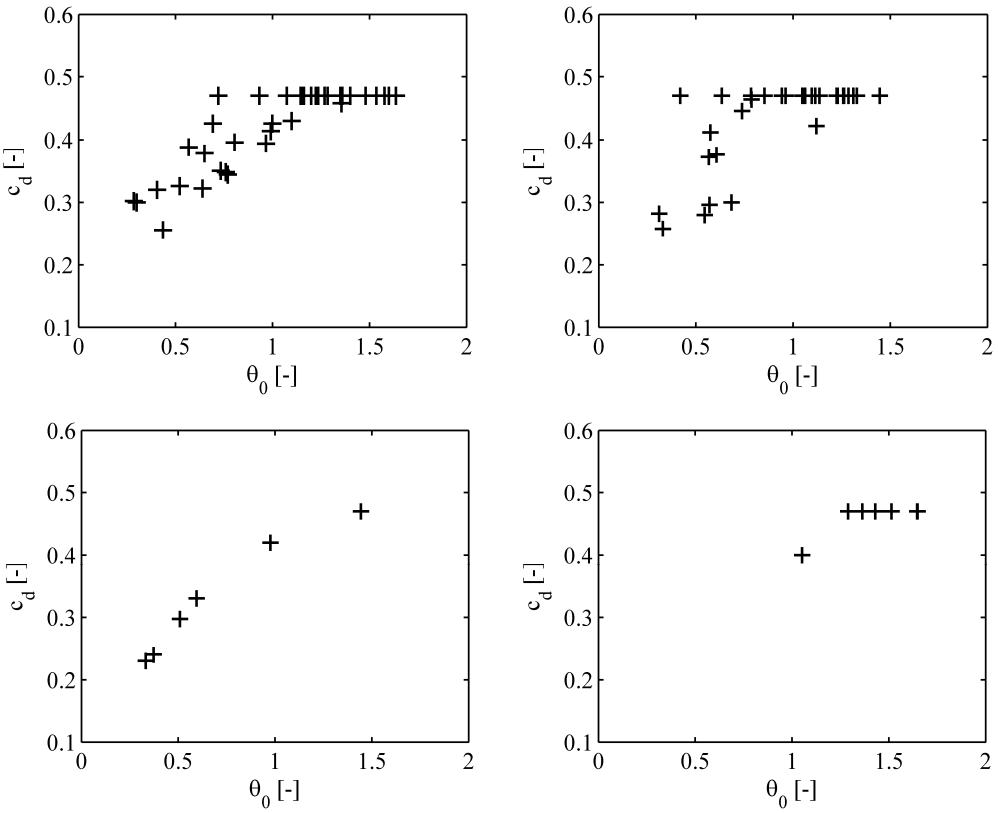

Fig. 3. Experimentally determined local concentration at bottom of collisional layer for flows of different bed Shields parameter (upper-left panel: TLT50, upper-right panel: TLT25, lower-left panel: FA60, lower-right panel: FA30).

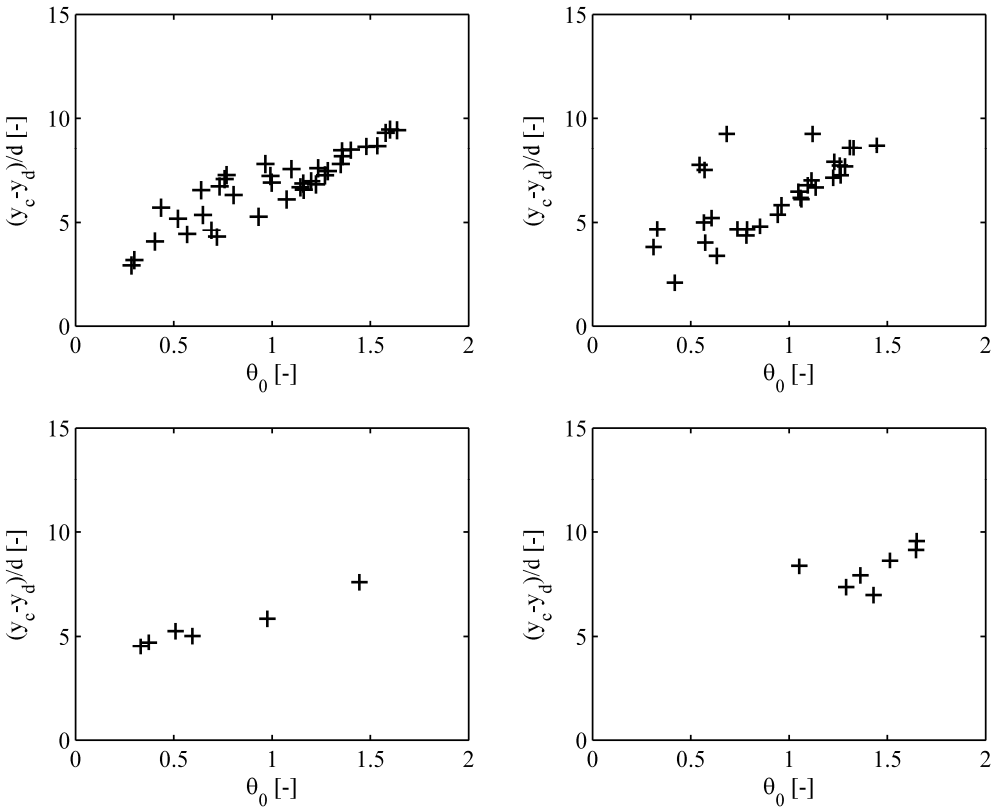

Fig. 4. Experimentally determined relative thickness of collisional layer (layer thickness divided by grain size) for flows of different bed Shields parameter (upper-left panel: TLT50, upper-right panel: TLT25, lower-left panel: FA60, lower-right panel: FA30).

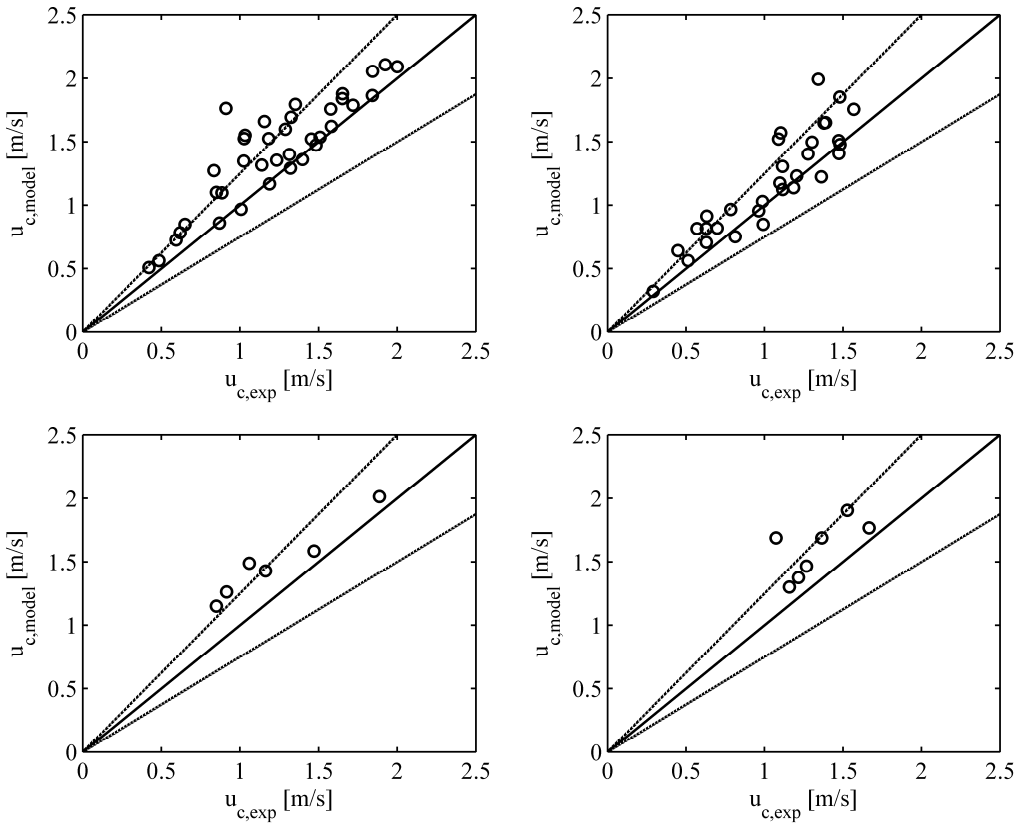

Fig. 5. Parity plot for experimental and predicted velocity at top of collisional layer. Legend: lines of perfect fit and of ± 25 per cent deviation. (upper-left panel: TLT50, upper-right panel: TLT25, lower-left panel: FA60, lower-right panel: FA30).

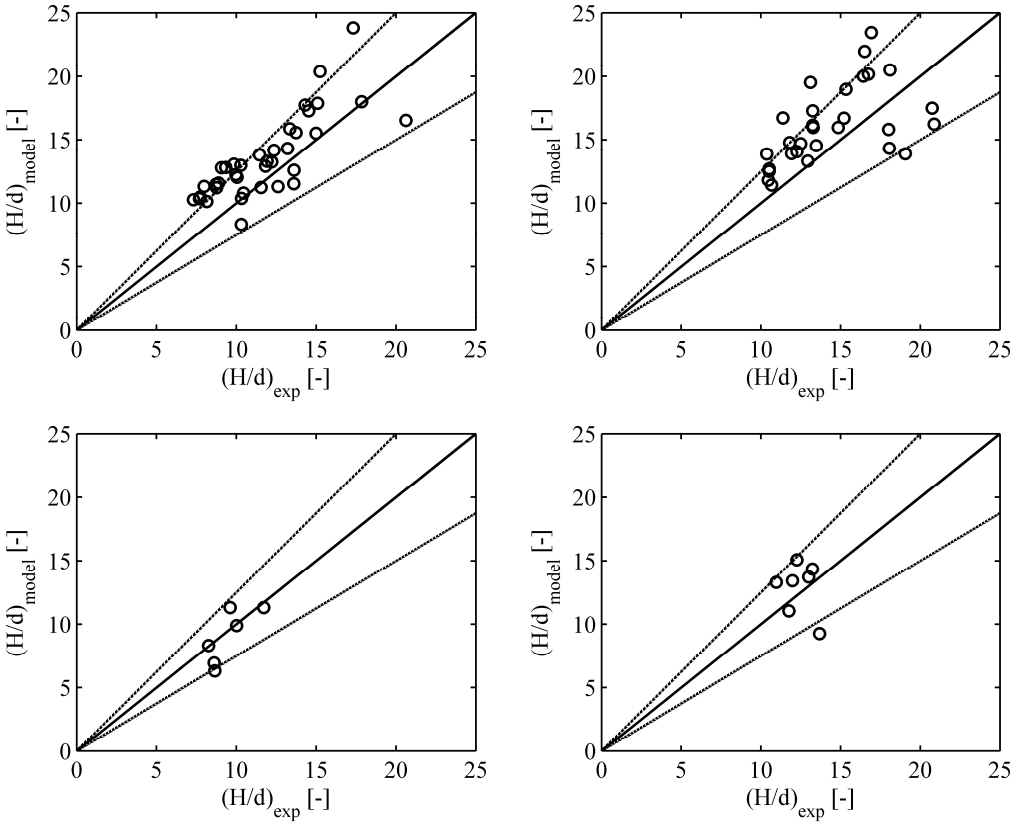

Fig. 6. Parity plot for experimental and predicted relative depth of flow (flow depth divided by grain size). Legend: lines of perfect fit and of ± 25 per cent deviation. (upper-left panel: TLT50, upper-right panel: TLT25, lower-left panel: FA60, lower-right panel: FA30).

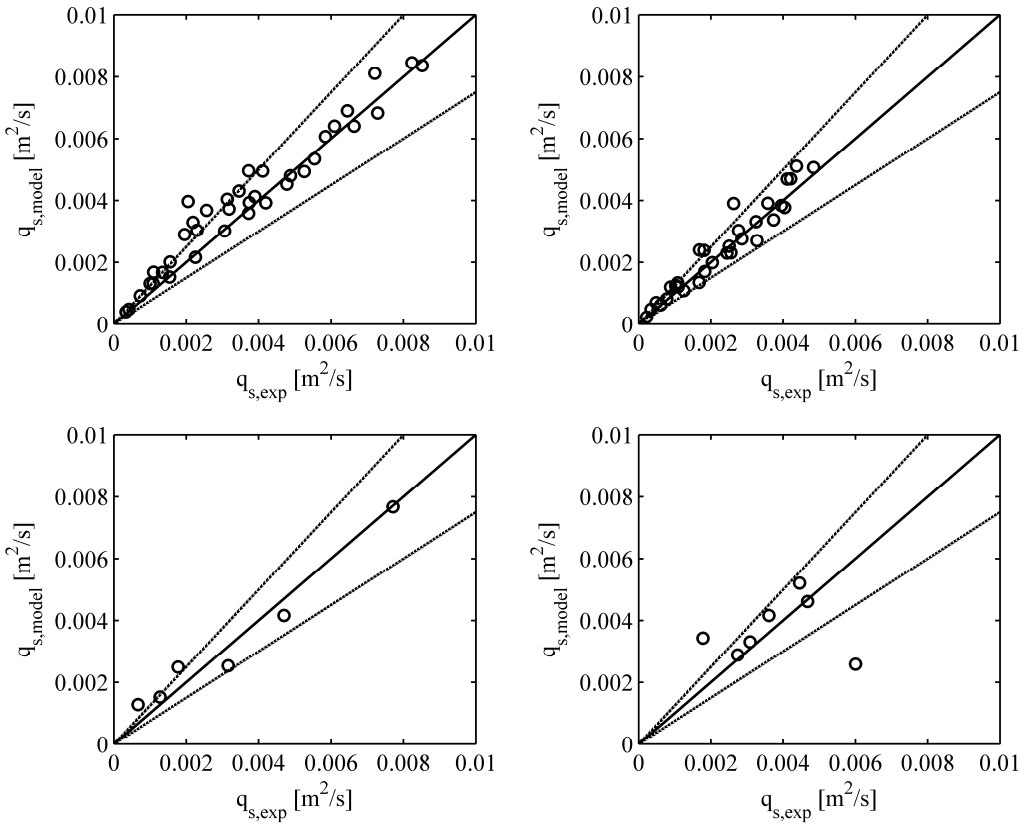

Fig. 7. Parity plot for experimental and predicted discharge of sediment (upper-left panel: TLT50, upper-right panel: TLT25, lower-left panel: FA60, lower-right panel: FA30). Legend: lines of perfect fit and of ± 25 per cent deviation.

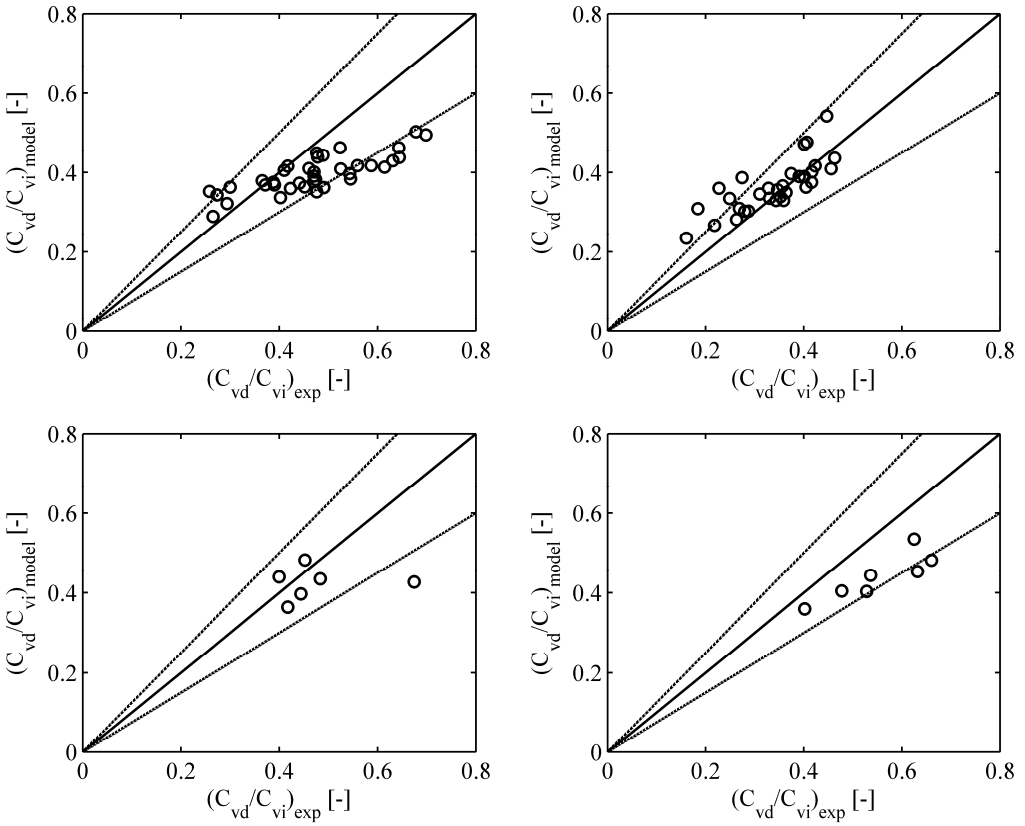

Fig. 8. Parity plot for experimental and predicted ratio of delivered concentration and spatial concentration of transported sediment (upper-left panel: TLT50, upper-right panel: TLT25, lower-left panel: FA60, lower-right panel: FA30). Legend: lines of perfect fit and of ± 25 per cent deviation.

CONCLUSIONS

A predictive model is presented for collisional bed load transport at high bed shear in an open channel. It employs constitutive relations of the classical kinetic theory previously selected as appropriate for transport and flow conditions under consideration on a basis of our laboratory testing. The model allows a prediction of the discharges of sediment and mixture for flows of given depth and longitudinal slope. Furthermore, it predicts the layered structure of the flow transporting bed load particles, giving the thickness of the collisional layer and the thickness of the sliding dense layer in the flow with intense bed load.

A comparison with experimental results for four fractions of lightweight model sediment suggests that the model reasonably predicts flow rates of both sediment and mixture at flow conditions observed in the laboratory tilting-flume experiment. Also, the predictions of the relation between the flow depth and the thickness of the collisional layer are satisfactory. The observed variation of the local concentration at the bottom of the collisional layer is considered in the model calculations.

Acknowledgement. The research has been supported by the Czech Science Foundation through the grant project No. 16-21421S. An assistance of J. Krupička and T. Picek with the experimental part of the research is highly acknowledged.

REFERENCES

Armanini, A., Capart, H., Fraccarollo, L., Larcher, M., 2005. Rheological stratification in experimental free-surface flows of granular-liquid mixtures. Journal of Fluid Mechanics, 532, 269–319.

Berzi, D., 2011. Analytical solution of collisional sheet flows. ASCE Journal of Hydraulic Engineering, 137, 10, 1200–1207.

Berzi, D., Fraccarollo, L., 2013. Inclined, collisional sediment transport. Physics of Fluids, 25, 106601.

Berzi, D., Fraccarollo, L., 2016. Intense sediment transport: Collisional to turbulent suspension. Physics of Fluids, 28, 023302.

Capart, H., Fraccarollo, L., 2011. Transport layer structure in intense bed-load. Geophysical Research Letters, 38, L20402.

Cheng, N.S., 2002. Exponential formula for bedload transport. ASCE Journal of Hydraulic Engineering, 128, 10, 942–946.

Garzo, V., Dufty, J.W., 1999. Dense fluid transport for inelastic hard spheres. Physical Review E 59, 5895–5911.

Jenkins, J.T., Hanes, D.M., 1998. Collisional sheet flows of sediment driven by a turbulent fluid. Journal of Fluid Mechanics, 370, 29–52.

Matoušek, V., Bareš, V., Krupička, J., Picek, T., Zrostlík, Š., 2016. Structure of flow with intense bed load layer. In: Proc. Int. Conf. River Flow 2016, Saint Louis, USA.

Matoušek, V., Zrostlík, Š., 2018a. Laboratory testing of granular kinetic theory for intense bed load transport. Journal of Hydrology and Hydromechanics, 66, 3, 330–336.

Matoušek, V., Zrostlík, Š., 2018b. Bed load transport modelling using kinetic theory. In: Proc. Int. Conf. River Flow 2018, Lyon, France.

Matoušek, V., Zrostlík, Š., 2019. Evaluation of local turbulent support of particles in intense transport of contact load. In: Proc. 19th Int. Conf. Transport & Sedimentation of Solid Particles, Cape Town, RSA.

Meyer-Peter, P., Müller, R., 1948. Formulas for bed-load transport. In: Report of 2nd Meeting of IAHSR, Stockholm, Sweden, pp. 39–64.

Rickenmann, D., 1991. Hyperconcentrated flow and sediment transport at steep slopes. ASCE Journal of Hydraulic Engineering, 117, 11, 1419–1439.

Smart, G.M., 1984. Sediment transport formula for steep channels. ASCE Journal of Hydraulic Engineering, 110, 3, 267–276.

Spinewine, B., Capart, H., 2013. Intense bed-load due to a sudden dam-break. Journal of Fluid Mechanics, 731, 579–614.

Wilson, K.C., 1966. Bed-load transport at high shear stress. Journal of Hydraulic Division ASCE, 92, 6, 49–59.

Wong, M., Parker, G., 2006. Reanalysis and correlation of bed-load relation of Meyer-Peter and Müller using their own database. ASCE Journal of Hydraulic Engineering, 132, 11, 1159–1168.

NOMENCLATURE

c_c – local volumetric concentration at top of collisional layer
c_d – local volumetric concentration at bottom of collisional layer
c_0 – local volumetric concentration at top of bed
d – particle diameter
e – coefficient of wet restitution
e_d – coefficient of wet restitution at bottom of collisional layer
f_s – concentration-related function
f_σ – concentration-related function
g – gravitational acceleration
q_m – total volumetric discharge of mixture
q_s – volumetric discharge of sediment
u – local velocities at different vertical positions
u_s – local velocity of solids
$u_{s,c}$ – velocity of solids at top of collisional layer
$u_{s,d}$ – velocity of solids at bottom of collisional layer
u_* – local liquid shear velocity
v_t – terminal settling velocity of grain
y – vertical position above top of bed
y_c – vertical position of top of collisional layer
y_d – vertical position of top of dense layer
C_{vd} – delivered concentration of sediment
C_{vi} – average spatial volumetric concentration of sediment in flow cross section
G – concentration-related function
H – total flow depth
T – local granular temperature
T_d – granular temperature at bottom of collisional layer
β_d – friction coefficient at bottom of collisional layer
β_0 – friction coefficient at top of bed
γ_s – local gradient of solids velocity
$\gamma_{s,d}$ – solids velocity gradient at bottom of collisional layer
ε – dry restitution coefficient
θ_0 – Shield parameter at top of bed
ρ_f – density of liquid
ρ_s – density of grains
μ_f – dynamic viscosity of liquid
ω – angle of longitudinal slope of bed
σ_s – local solids normal stress
$\sigma_{s,d}$ – solids normal stress at top of dense layer
$\sigma_{s,0}$ – solids normal stress at top of bed
τ_e – local total shear stress
$\tau_{e,d}$ – total shear stress at top of dense layer
τ_f – local liquid shear stress
τ_s – local solids shear stress
$\tau_{s,d}$ – solids shear stress at top of dense layer

Received 2 September 2019
Accepted 9 December 2019